NANO LETTERS

LETTER

pubs.acs.org/NanoLett

Negative and Positive Persistent Photoconductance in Graphene

Chandan Biswas,[†] Fethullah Güneş,[†] Duong Dinh Loc ,[†] Seong Chu Lim,[†] Mun Seok Jeong,[‡] Didier Pribat,[†] and Young Hee Lee*[,†]

[†]SKKU Advanced Institute of Nanotechnology, WCU Department of Energy Science, Department of Physics, Graphene Center, Sungkyunkwan University, Suwon 440-746, Republic of Korea

[‡]Advanced Photonics Research Institute, Gwangju Institute of Science and Technology, Gwangju 500-712, Republic of Korea

Supporting Information

ABSTRACT: Persistent photoconductance, a prolonged light-induced conducting behavior that lasts several hundred seconds, has been observed in semiconductors. Here we report persistent negative photoconductance and consecutive prominent persistent positive photoconductance in graphene. Unusually large yields of negative PC (34%) and positive PC (1652%) and remarkably long negative transient response time (several hours) were observed. Such high yields were reduced in multilayer graphene and were quenched under vacuum conditions. Two-dimensional metallic graphene strongly interacts with environment and/or substrate, causing this phenomenon, which is markedly different from that in three-dimensional semiconductors and nanoparticles.

KEYWORDS: Graphene, positive photoconductance, negative photoconductance, persistent photoconductance, optoelectronics

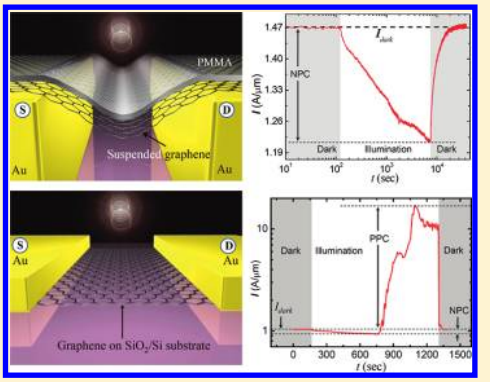

Graphene, a single layer of two-dimensional honeycomb carbon lattices, exhibits numerous exotic behaviors such as the anomalous quantum Hall effect,[1] the Klein paradox,[2] and coherent transport.[3] In contrast, optoelectronic, excitonic, and/or impurity related electron dynamics studies are limited despite its scientific and technical relevance. Persistent photoconductance,[4−6] a prolonged light-induced conducting behavior over several hundred seconds, has often been observed in three-dimensional semiconductors with high impurity or in functionalized nanoparticles.[6] Illuminating light generates mobile charge carriers in the valence and/or conduction bands of the traditional photoconductors,[4−11] resulting in increased conductivity.[7] Such positive photoconductance (PPC) was observed in both bulk and nanostructured photoconductors.[6,8] In contrast, conductivity could decrease by light excitation (negative photoconductivity, NPC) in doped III−V semiconductors,[9,10] diamond thin films,[11] quantum well heterostructures,[4] and metal nanoparticles.[6] Impurity-related photoabsorptions allowing electronic transitions between localized or extended states have been employed to explain the above phenomena. The existence of NPC in metals and simultaneous observation of persistent NPC and PPC have not been observed. Enhancement of such effects could be advantageous in numerous optoelectronic devices and is expected to be observed in low-dimensional systems. Here we report persistent NPC in suspended graphene and a successive persistent NPC, followed by a prominent substrate induced persistent PPC in graphene on SiO_2 substrate. The yield and transient response time (over several hours) of photoconductance change upon light illumination distinct from conventional photodetectors[4−11] and were unusually large in monolayer graphene, although this effect was reduced significantly as the number of graphene layers increased. Two-dimensional semimetallic graphene shows these behaviors due to its planar structure, in which the constituent atoms are exclusively exposed to the ambient, resulting in strong interactions with the environment and/or substrate. These phenomena could not be observed in conventional three-dimensional metal or semiconductor structures due to their bulk natures which differ significantly from an ideal two-dimensional graphene structure.

Monolayer graphene was transferred onto SiO_2/Si substrate and two Au electrodes were formed for source and drain (inset of Figure 1a). A constant dark current (I_{dark}) was observed at a fixed source−drain voltage, V_{SD} = 10 mV under ambient conditions (Figure 1a,b). Monochromatic light illumination (200 nm wavelength) onto the device gradually decreases the current level over a prolonged time of 700 s. This phenomenon is called persistent NPC. Subsequently, a rapid increase in current (at point a) reached to a maximum value (point c) in about 300 s of time scale, called a persistent PPC. Four distinct regions were observed during transient current measurement under light illumination: a, transition time from NPC to PPC region; b, an intermediate bump; c, maximum current peak; d, saturated current region (PPC_{sat}). The formation of an intermediate bump, an overshoot maximum current, and subsequent current saturation were consistently observed independent of the incident light wavelengths. Thus, the single-layer graphene films transferred on SiO_2/Si substrate exhibited persistent NPC and PPC behaviors simultaneously, which have not been observed previously.

Received: July 5, 2011
Revised: September 19, 2011
Published: October 05, 2011

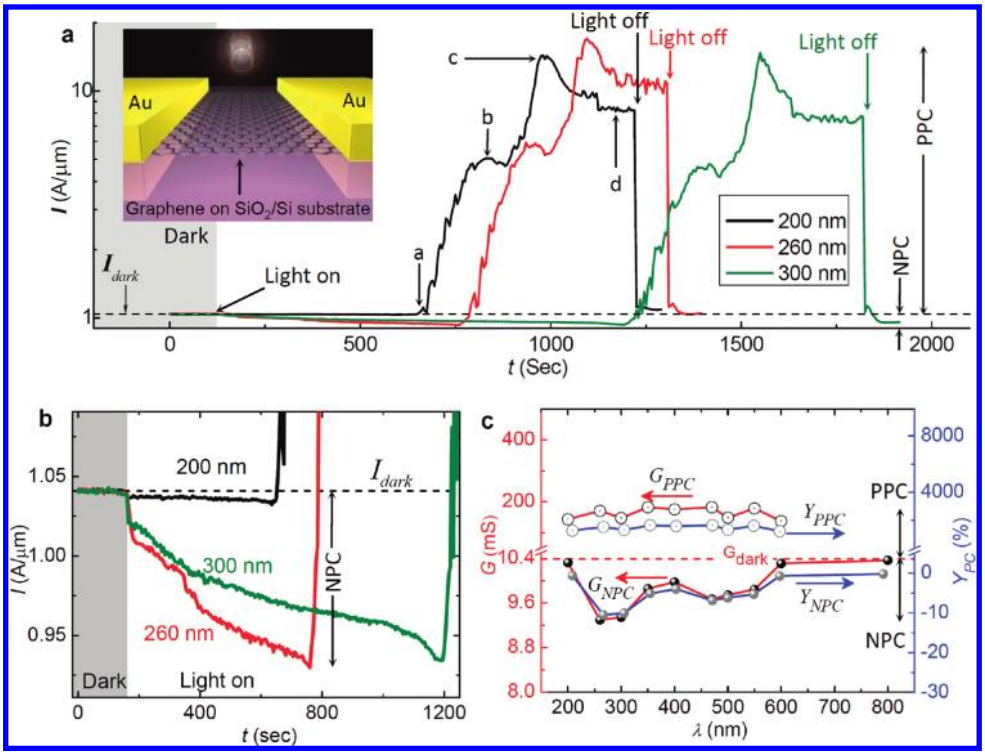

Figure 1. Positive and negative photoconductance in graphene deposited on SiO_2 substrate. (a) Transient photoresponse of a monolayer graphene transferred on to a SiO_2/Si wafer (300 nm thick silica) under different illuminated light wavelengths, followed by source and drain Au electrode deposition with a 1 mm channel length and 1 cm channel width (inset). Without light impregnation, the device shows constant current density (I_{dark}) at a fixed 10 mV bias, while light illumination decreases current persistently (from I_{dark} to point a). The current is normalized with respect to the channel width. The current then persistently produces much higher I_{dark} values with two characteristic peaks at points b and c, until it becomes saturated at point d. Light extinguishment at this stage results in a sharp decrease in the current back to a level close to that of the I_{dark} level. (b) A magnified region of panel A highlights the maximal NPC values at 260 nm illumination. (c) Changes in device conductance, G, and calculated photoconductance yield, Y_{PC} (the change in current due to photon irradiation with respect to I_{dark}, $(I - I_{dark})/(I_{dark}) \times 100$), with irradiated light wavelength. The values of G and Y_{PC} are denoted as G_{PPC} and Y_{PPC} for PPC and as G_{NPC} and Y_{NPC} for NPC, respectively. All current measurements were normalized according to the monochromatic light intensities for comparison.

Figure 1b shows the magnified NPC region of Figure 1a, in which NPC is clearly distinguishable among the different light wavelengths. The largest NPC was observed at 260 nm (4.77 eV). The transition time was extended with increasing light wavelengths. More detailed observations of graphene conductance (G) and photoconductivity yield ($Y_{PC} = (I - I_{dark})/I_{dark}$) in terms of light wavelength are represented in Figure 1c. The dark conductance was 10.3 mS, which is the largest among the existing graphene layers.[3] The maximum NPC (NPC_{max}) yield of 10.5% ($Y_{PC} = -10.5\%$) was obtained near 260 nm. On the other hand, no NPC yield was observed at long wavelength near 800 nm. In contrast, a large yield in PPC in the range of 1200−1650% was observed and was about 100 times larger than that of NPC, where the values fluctuated within 25% at different illuminated wavelengths.

To eliminate the oxide substrate effect, another set of experiments was performed with a suspended graphene. A 500 nm thick insulating transparent PMMA[12] thin film was used as a mechanical support of the graphene layer (Figure 2a). The dark conductance of monolayer graphene (G_{dark}) was further increased to 14.7 mS (at 10 mV bias) by removing the substrate scattering in the graphene channel. Upon light illumination, the current level decreased exponentially and was saturated in a long time scale of a few hours, demonstrating persistent NPC (Figure 2b). The saturated currents relied strongly on the excited wavelengths (Figure 2c). A maximum NPC yield ($Y_{NPC} = 34\%$) was also observed near 260 nm, and negligible NPC yield was observed at a long wavelength of 1000 nm (Figure 2c, Figure S3A in the Supporting information). This phenomenon correlated with the light absorption by graphene at lower wavelength regions.[13] The NPC_{max} yield of suspended graphene was about 3 times larger than that of SiO_2 substrate with similar wavelength variations. The disappearance of the PPC regions was evident in suspended graphene and independent of the wavelength of the incident light even after several hours of exposure time. The yield was linearly proportional to the power of the input light source (Figure S4G, Supporting Information). This indicates that the phenomena are intrinsically material-related optical properties unlike nonlinear optics.[14] The device was placed into a vacuum chamber at 20 mTorr pressure to investigate the changes in photoresponse (Figure 2d). The dark conductance level (originally p-type) was reduced to 6.54 mS compared to ambient measurements (14.7 mS), which was attributed to the desorption of adsorbates under vacuum (Figure S3G, Supporting Information). The NPC_{max} remained constant at 260 nm light exposure. However, the NPC yield was reduced to 10.5% (inset in Figure 2d) compared to the ambient (34%). The sample was further annealed under vacuum at 200 °C for 4 h. No appreciable changes in current were observed under light illumination at any wavelength. Fluctuations in the current were less than 0.2%

dx.doi.org/10.1021/nl202266h |Nano Lett. 2011, 11, 4682–4687

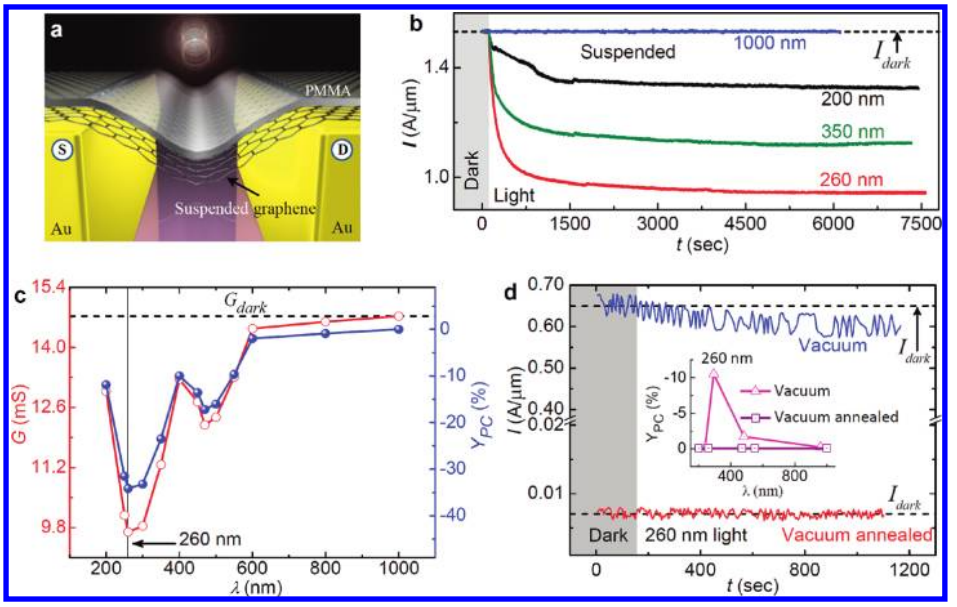

Figure 2. Persistent negative photoconductance in a suspended graphene device. (a) Schematic diagram of the suspended graphene device connected by source and drain gold electrodes. The PMMA layer was used as a mechanical support between the two electrodes. (b) Transient current dynamics at a constant applied bias (10 mV) under different monochromatic light irradiation (from 200 to 1000 nm) in a monolayer of graphene suspended between two biasing electrodes. The current on the graphene channel decreases upon light irradiation (NPC) compared to I_{dark} and is saturated over a long time scale. (c) G and Y_{PC} in the device depend on the illumination wavelength and show maximum NPC yield at 260 nm light illumination. (d) Transient current response of the same device at 10 mV bias in dark and 260 nm illumination in vacuum (20 mTorr) and after vacuum annealing (at 200 °C for 4 h). The inset represents the NPC yield variations at different illumination wavelengths. All current measurements are normalized according to the monochromatic light intensity.

(Figure 2d) and were independent of the illuminated light wavelength, indicating complete extinction of NPC behavior from the monolayer of suspended graphene.

The observed persistent NPC was strongly related to the surface adsorbates. To observe this phenomenon more clearly, the suspended graphene devices were fabricated with different numbers of graphene layers. The general trend in NPC_{max} near 260 nm and suppression of the yield at long wavelengths were similar even for multilayer graphene devices (Figure 3a, Figure S3 in the Supporting Information). However, the absolute value of NPC yield (Y_{NPC}) was drastically reduced as the number of layers increased. The dark conductance of the pristine monolayer graphene (G_{dark}) under ambient conditions was 14.7 mS (Figure 3b). This value was reduced under vacuum (6.54 mS) and was further reduced (70.7 μS) under vacuum annealing (Figure S3, Supporting Information). The conductance increased gradually as the number of layers increased. With four graphene layers, the conductance reached to 50.8 mS. However, the NPC yield (at NPC_{max}) was reduced to 7.2% in two layers and 2% with four layers compared to 34% of the monolayer case. The decrease of the NPC yield originated from the diminished surface effect in the multilayer device. Current saturation time (t_{satu}) during NPC was also compared for different layers (Figure S4D, Supporting Information). The NPC saturation time was 7560 s for the single layer and decreased as the number of layers increased. This again confirmed that the NPC phenomena were ascribed to the surface adsorbates.

The effects of different substrates on the maximum photoconductance yield were also investigated by using a monolayer graphene device (Figure 3c). The suspended graphene had the largest NPC yield among other substrates used in this study. The NPC yield was reduced from SiO_2/Si substrate from 34% to 10.5%. Other types of substrates, such as SiO_2-coated polyethylene–terephthalate (PET) and PET substrates provided similar NPC yields to that of SiO_2/Si substrate. Similar transient photoresponses were also observed from other substrates (see Figure S5A, Supporting Information). No PPC phenomenon was observed except in the SiO_2/Si substrate. This unique observation of prominent PPC from the SiO_2/Si substrate does not result exclusively from the SiO_2 layer but was also associated with the Si substrate, since no PPC was observed from the SiO_2/PET substrate. The possibility of leakage current contribution during light illumination was excluded due to constant low leakage current observations (see Figure S5B, Supporting Information) simultaneously observed during photocurrent measurements.

Several questions arose from these observations regarding (i) the origins of NPC and PPC, (ii) the maximum NPC yield at 260 nm, (iii) the simultaneous existence of both NPC and PPC on the SiO_2/Si substrate, and (iv) the strong layer dependence of photoconductance yield. One common feature was that both PPC and NPC were the adsorbent-sensitive surface effects. Here we show band structure of pure graphene with the band gap at each K point (Figure 4a). From Γ to M the band gap is opened with a minimum 4.77 eV (260 nm), while a continuous energy difference from the maximum valence and to the minimum conduction band exists from Γ to K. The origin of the maximum NPC yield at 260 nm is closely related to the absorption of UV light near the M point of the graphene band structure.[13,15] The maximum light absorption was obtained due to the large electron density of states at the M point (Figure 4b). In addition to this, light will be absorbed constantly near the K point, but the electron density of states is relatively low around this region, producing less photogenerated carriers. The strong light absorption could be also related to the π-plasmon resonance of few

dx.doi.org/10.1021/nl202266h |*Nano Lett.* 2011, 11, 4682–4687

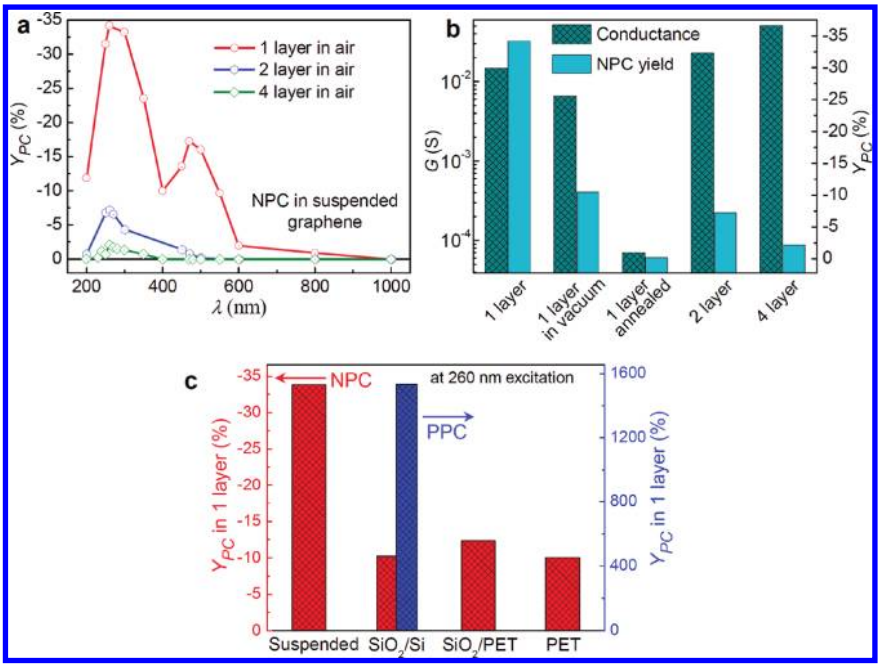

Figure 3. Photoconductance variations with multilayer graphene and different substrates. (a) NPC yield variations of the suspended graphene devices at different illuminated light wavelengths. All devices show NPC_{max} at 260 nm light excitation. (b) Comparisons of the absolute values of G and NPC yields of the suspended graphene devices at 260 nm light irradiation (10 mV applied bias). Conductance and NPC yield of the single layer were reduced under vacuum compared to that at ambient. Device conductance increased in the multilayer, although NPC yield still decreased under ambient conditions. (c) The Y_{PC} of NPC and PPC (at NPC_{max} with 260 nm light excitation) of monolayer suspended graphene with a single layer transferred onto a different substrate. Only the SiO_2/Si device shows both simultaneous NPC and PPC behavior, while all other devices show only NPC behavior. The NPC yield in the suspended device was the highest among all of the devices.

layers of graphene. In general, the π-plasmon energy is layer-dependent, 7 eV for 10 layers and 4.8 eV for monolayer graphene.[16] In our case, however, NPC_{max} remained unchanged at 260 nm light excitations for different numbers of graphene layers (Figure S3C−F, Supporting Information). This excludes the possibility of plasmonic absorption.

Despite such abundant photogenerated carriers in graphene, these carriers do not give rise to persistent photoconductivity due to the fast recombination process in the pure graphene layer in the absence of adsorbates. In order to understand the NPC behavior in graphene and its correlation with absorbents on its surface, the theoretical electronic density of states (DOS) was calculated, along with partial density of states (PDOS) of oxygen, hydroxyl (OH), oxygen atom, and water absorbents on graphene surface (Figure 4b,c, Figure S6 in the Supporting Information). O_2 molecules can be physisorbed on the hexagonal site of graphene with a binding energy of 20 meV. This donates electrons to graphene and shifts the Fermi level by 0.5 eV (Figure 4b). The O_2 molecular state is half-filled or pinned at the Fermi level. A similar pinning effect is observed in the case of OH adsorption. In this case, OH is strongly chemisorbed with a binding energy of 0.56 eV. Most of the OH levels are occupied states located within the valence band. Other types of adsorbents such as the oxygen atom and H_2O molecules showed no localized states (Figure S6, Supporting Information). These strongly localized states formed by either O_2 and/or OH groups act as scattering centers for free carriers.[17] These adsorbents may be formed on the graphene surface under ambient conditions, which act as scattering centers under light illumination and reduce the conductance of the device and, hence, are the origin of NPC. The presence of oxygen-related functional groups was confirmed using XPS analysis (Figure S2, Supporting Information). Sample annealing under vacuum removes these adsorbents, and the related NPC phenomenon disappeared.

The original graphene device is p-type due to the presence of oxygen-related functional groups on the graphene surface.[18,22] The localized oxygen/hydroxyl related impurity states at the Fermi level increase the charge scattering of the hole carriers, which invokes the NPC phenomenon (Figure 4di and dii). In the case of the SiO_2/Si substrate, positive charge trap sites exist at the interface of graphene/SiO_2 and SiO_2/Si.[18,19] These trap sites are additional scattering centers for carriers (Figure 4diii). Therefore, the dark current should be reduced compared to that of the suspended graphene device. This argument was confirmed via our experiment which showed that the dark current of the pristine suspended graphene device was 1.47 A/μm (current flow per graphene channel width), larger than 0.43 A/μm with the SiO_2 substrate (Figures 1b and 2b). With light excitation, NPC was invoked by impurity scattering on the graphene surface and trap charges at the interfaces of graphene/SiO_2 and SiO_2/Si. Simultaneously, photogenerated charge carriers in the silicon substrate neutralize the positive trap charges at the SiO_2/Si interface.[19] This reduces trap charge scattering and therefore suppresses the reduction of the current, limiting large NPC. When the effect of trap charge neutralization competes with impurity charge scattering on graphene, a transition starts to occur (point a in Figure 1a). As the neutralization of trap charges proceeds, the scattering from the interface charges becomes less effective, and the photogenerated carriers begin to contribute to the positive current. The presence of two peaks in the positive current region (points b and c) could be related to the existence of trap charges at two interfaces of graphene/SiO_2 and SiO_2/Si.

dx.doi.org/10.1021/nl202266h |*Nano Lett.* 2011, 11, 4682–4687

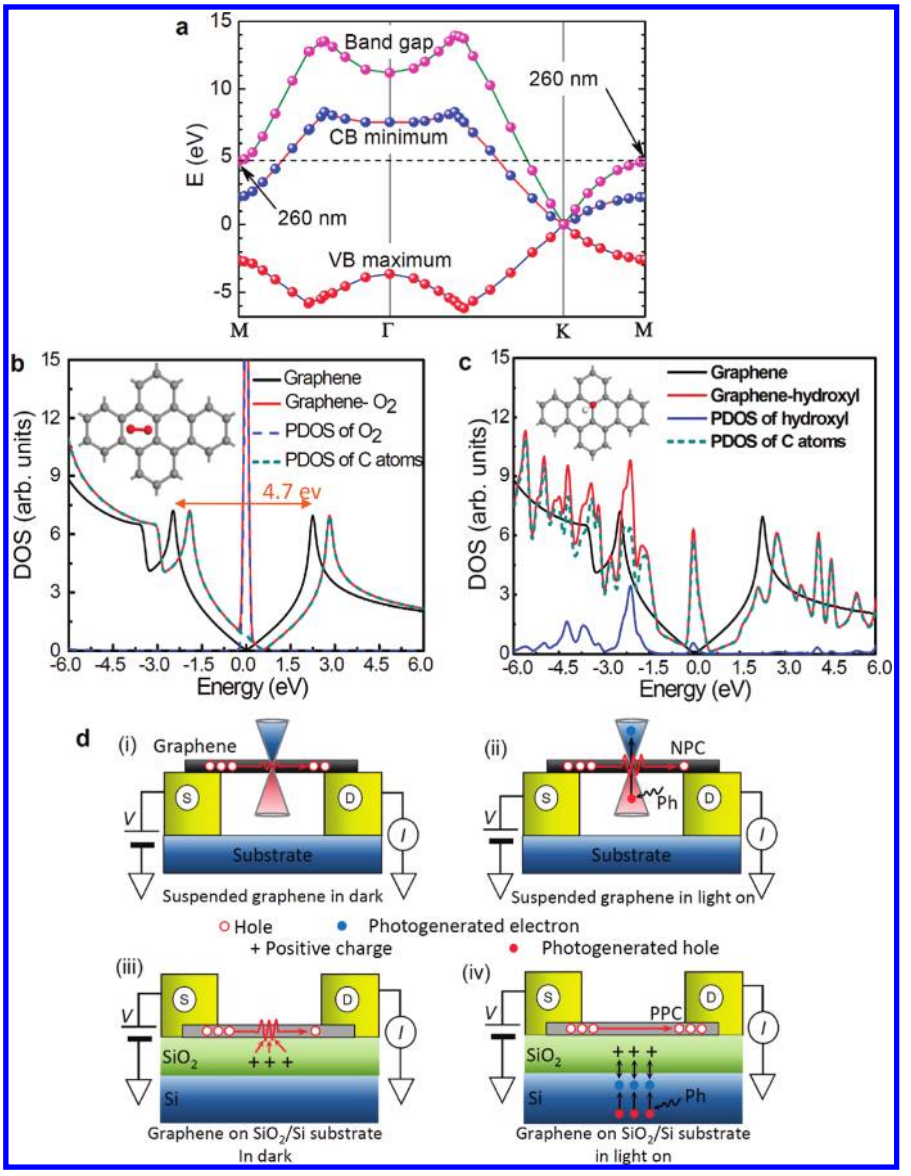

Figure 4. Absorbents dependent photoconductance in graphene. (a) Calculated conduction band minimum, valence band maximum, and corresponding band gap at different K spaces of the pure graphene monolayer containing two atoms. The calculation was fabricated using the local density approximation (LDA) method. (b, c) Comparisons of electronic density of states (DOS) and partial density of states (PDOS) of the pure graphene monolayer (containing 24 carbon atoms per unit cell, GGA method) with an oxygen- (B), and hydroxyl-doped (C) (one oxygen, hydroxyl molecule per unit cell shown in figure insets) graphene monolayer. The Fermi level of graphene is located at zero energy. (d) (i) Schematic diagram of the suspended graphene device and its current measurements in the dark represents only intrinsic graphene resistance during carrier conductions in the channel. (ii) Under light conditions, the conductivity of graphene decreases due to the scattering between free and photogenerated charge carries at absorbent sites, producing an NPC effect. (iii) Schematic representation of graphene's reduced conductivity (transferred on to the SiO_2/Si substrate) due to charge impurity scattering the from SiO_2 substrate in the dark. (iv) Under light illumination, photogenerated electrons in the Si substrate neutralize the positive charges from the SiO_2, resulting in increments in graphene photoconductivity and PPC behavior.

After filling up all of the charged trap sites, the conductance reaches to a maximum (point c). The continuously generated photogenerated carriers can be overshot due to the excess kinetic energy and then cooled to saturate the final equilibrium current (point d). The mobility (and corresponding conductance) of the graphene device could be increased by reducing the number of charged impurities particularly in the case of the SiO_2/Si substrate.[18,20,21] The presence of PPC behavior was only observed in the SiO_2/Si substrate due to the dominant trap site reduction in SiO_2 that occurs due to the photoexcited charge carrier generation in the Si substrate and could not be repeatable in SiO_2/PET or PET substrate. Photoexcited free charge carrier dynamics and its interactions with charged substrate could be highlighted by controlling the carrier types in graphene and need to be investigated in the future. Photocurrent measurements obtained using a scanning photocurrent microscope correlate with only the local band bending near the photoexcited laser spot and do not represent the net conductance changes under light illumination covering the whole channel area and hence could not be compared with the observed phenomenon here.[22] Layer dependence can be also explained by the dominant adsorbent effect on the graphene surface. In the case of a multilayer graphene device, the conductance was contributed from several graphene layers in

dx.doi.org/10.1021/nl202266h |*Nano Lett.* 2011, 11, 4682–4687

parallel including the surface layer. However, the adsorbate (oxygen/hydroxyl) related impurity was dominant only in the surface layer of graphene and very negligible in the unexposed layers underneath. Photoinduced impurity scattering was dominant only on the surface layer. However, the conduction through the graphene layers beneath the surface layer was unaffected by the photoinduced impurity charge scattering. This thus reduces the NPC effect.

The simultaneous observation of persistent NPC and PPC from graphene was associated with not only the SiO_2/Si substrate but also adsorbent-sensitive graphene due to its ideal 2D structure, which has never before been reported in a 3D structure. This opens up a new field to understand photoexcited optoelectronic carrier dynamics in 2D structures such as graphene and BN. These new properties of graphene could be utilized in future optoelectronic devices such as photosensors, optical switches, and solar cells.

■ ASSOCIATED CONTENT

Supporting Information. Details of materials and methods, further discussion, and supporting figures. This material is available free of charge via the Internet at http://pubs.acs.org.

■ AUTHOR INFORMATION

Corresponding Author
*E-mail: leeyoung@skku.edu.

■ ACKNOWLEDGMENT

This work was supported by the Star Faculty program (2010-0029653), International Research & Development Program (2011-00242), and WCU program (R31-2008-10029) of the NRF of Korea funded by MEST. We acknowledge Philip Kim and Atul Kulkarni for their critical comments and valuable contributions on the manuscript.

■ REFERENCES

(1) Zhang, Y. B.; Tan, Y. W.; Stormer, H. L; Kim, P. *Nature* **2005**, *438*, 201–204.
(2) Katsnelson, M. I.; Novoselov, K. S.; Geim, A. K. *Nat. Phys.* **2006**, *2*, 620–625.
(3) Miao, F.; Wijeratne, S.; Zhang, Y.; Coskun, U. C.; Bao, W.; Lau, C. N. *Science* **2007**, *317*, 1530–1533.
(4) Chaves, A. S.; Chacham, H. *Appl. Phys. Lett.* **1995**, *66*, 727–729.
(5) Kulbachinskii, V. A.; Kytin, V. G.; Golikov, A. V.; Lunin, R. A.; Schaijk, R. T. F. V.; Visser, A. D.; Senichkin, A. P.; Bugaev, A. S. *Semicond. Sci. Technol.* **2000**, *15*, 895–901.
(6) Nakanishi, H.; Bishop, K. J. M.; Kowalczyk, B.; Nitzan, A.; Weiss, E. A.; Tretiakov, K. V.; Apodaca, M. M.; Klajn, R.; Stoddart, J. F.; Grzybowski, B. A. *Nature* **2009**, *460*, 371–375.
(7) Joshi, N. V. *Photoconductivity: Art, Science and Technology*; Marcel Dekker: New York, 1990.
(8) Hayden, O.; Agarwal, R.; Lieber, C. M. *Nat. Mater.* **2006**, *5*, 352–356.
(9) Wei, P.-C.; Chattopadhyay, S.; Yang, M.-D.; Tong, S. C.; Shen, J. L.; Lu, C. Y.; Shih, H. C.; Chen, L. C.; Chen, K. H. *Phys. Rev. B* **2010**, *81*, 045306.
(10) Raichev, O. E.; Vasko, F. T. *Phys. Rev. B* **2006**, *73*, 075204.
(11) Liao, M.; Koide, Y.; Alvarez, J.; Imura, M.; Kleider, J.-P. *Phys. Rev. B* **2008**, *78*, 045112.
(12) Jana, S.; Salehi-Khojin, A.; Zhong, W.-H.; Chen, H.; Liu, X.; Huo, Q. *Solid State Ionics* **2007**, *178*, 1180–1186.
(13) Wang, Y.; Ni, Z.; Liu, L.; Liu, Y.; Cong, C.; Yu, T.; Wang, X.; Shen, D.; Shen, Z. *ACS Nano* **2010**, *4*, 4074–4080.
(14) Sze, S. M. *Physics of Semiconductor Devices*, 2nd ed.; Wiley: New York, 1981.
(15) Yang, L.; Deslippe, J.; Park, C.-H.; Cohen, M. L.; Louie, S. G. *Phys. Rev. Lett.* **2009**, *103*, 186802.
(16) Eberlein, T.; Bangert, U.; Nair, R. R.; Jones, R.; Gass, M.; Bleloch, A. L.; Novoselov, K. S.; Geim, A.; Briddon, P. R. *Phys. Rev. B* **2008**, *77*, 233406.
(17) Ouyang, Y.; Sanvito, S.; Guo, J. *Surf. Sci.* **2010**, DOI: 10.1016/j.susc.2010.10.030.
(18) Chen, J. H.; Jang, C.; Adam, S.; Fuhrer, M. S.; Williams, E. D.; Ishigami, M. *Nat. Phys.* **2008**, *4*, 377–381.
(19) Shi, Y.; Dong, X.; Tantang, H.; Weng, C. H.; Chen, F.; Lee, C.; Zhang, K.; Chen, Y.; Wang, J.; Li, L. J. *J. Phys. Chem. C* **2008**, *112*, 18201–18206.
(20) Morozov, S. V.; Novoselov, K. S.; Katsnelson, M. I.; Schedin, F.; Elias, D. C.; Jaszczak, J. A.; Geim, A. K. *Phys. Rev. Lett.* **2008**, *100*, 016602.
(21) Bolotin, K. I.; Sikes, K. J.; Jiang, Z.; Klima, M.; Fudenberg, G.; Hone, J.; Kim, P.; Stormer, H. L. *Solid State Commun.* **2008**, *146*, 351–355.
(22) Park, J.; Ahn, Y. H.; Ruiz-Vargas, C. *Nano Lett.* **2009**, *9*, 1742–1746.